Carolina Manresa
Manel Bosch
María Cristina Manzanares
Patricia Carvalho
José Javier Echeverría

Short Communication

A new standardized-automatic method for bone-to-implant contact histomorphometric analysis based on backscattered scanning electron microscopy images

Authors' affiliations:
Carolina Manresa, José Javier Echeverría,
Departament d'Odontoestomatologia, Odontologia
Integrada d'Adults, Facultat d'Odontologia,
Universitat de Barcelona, Barcelona, Spain
Manel Bosch, Unitat de Microscòpia Òptica
Avançada, Centres Científics i Tecnològics de la
Universitat de Barcelona (CCiTUB), Barcelona,
Spain
María Cristina Manzanares, Patricia Carvalho,
Human Anatomy and Embryology Unit, DPyTEx,
Health Universitat de Barcelona Campus (HUBc),
Barcelona, Spain

Corresponding author:
Carolina Manresa
Facultat d'Odontologia
Campus de Bellvitge
Universitat de Barcelona
Feixa Llarga
s/n, 08907 L'Hospitalet de Llobregat
Barcelona, Spain
Tel.: (+34) 93 4024289
Fax: (+34) 93 4024248
e-mail: cmanresa@ub.edu

Key words: animal experiments, bone–implant interaction, morphometric analysis

Abstract
Aim: To establish an image analysis procedure for measuring the bone-to-implant contact (BIC) by a systematic non-subjective approach based on backscattered scanning electron microscopy (BS-SEM) images.
Material and methods: A total of 36 dental implants (9 mm length, Ø 4.0 mm with a SBM surface) were implanted in six beagle dog mandibles. The implants were removed after 1, 2, 4, 6, and 8 weeks and then embedded in resin and cut along their long axis. Sample observation was performed by BS-SEM, acquiring 10 to 16 images per sample. Image processing and BIC determination were performed using the Fiji image processing package. Images were stitched, filtered, and thresholded to obtain a binary image of the whole implant that finally was dilated and outlined. The length of this outline was measured as the maximum possible BIC. The regions of coincidence between this line and the bone were measured as the real BIC.
Results: The proposed methodology for BIC determination, based on SEM, which has a much higher resolution than optical microscopy, allows the acquisition of highly discriminative images with great contrast between implant and bone. The high resolution and high contrast in SEM images provide more accurate results than those obtained by classical methods. Furthermore, the methodology of image analysis described in this study delineates precisely and automatically the contour of the implant, which results in non-biased measurements. The average percentage of BIC was 35%, ranging from 24.7 to 45.5%. These values were similar to the results documented in the literature for implants of similar roughness in animal models.
Conclusions: A novel, non-subjective, and systematic method for measuring BIC is described based on BS-SEM images. The proposed methodology minimizes the shortcomings of the results obtained by previously described methods.

The evaluation methods of osseointegration could be categorized as invasive or non-invasive, by evaluating the implant *in situ* (*in vivo*) or *ex situ* (*ex vivo*) from the patient or experimental animals, respectively. The evaluation of *in vivo* functional implants is limited to different X-ray and resonance frequency methods. The most common methods for evaluation of retrieved implants (*ex vivo*) and surrounding tissue include the following: biomechanical tests, such as push or pull out or torque tests, and light microscopy, confocal laser scanning microscopy (CLSM), and scanning electron microscopy (SEM) observation of blocks, including the implant and surrounding tissues.

The histological assessment of bone adjacent to dental implants is mostly performed using variations of the sawing and grinding technique described by Donath & Breuner (1982) and the evaluation of stained thin sections by light microscopy. This is the standard methodology widely used for the determination of the histomorphometric parameter BIC% (percentage of bone-to-implant contact), which is defined as the percentage of implant length at which there is direct bone contact, without intervening fibrous tissue.

The drawbacks of the classical procedure, based on light microscopy, include need for staining, low resolution, time-consuming

laboratory procedures, and the risk of bias in the microscopic evaluation. BIC determination by this methodology is performed in most cases, by drawing the line manually where the measurement is to be performed. In others studies, however, some digital image processing and analysis are carried out, but a well-defined workflow of image analysis is still lacking, and too much subjectivity could influence the final results. It would be desirable to have a simpler, highly discriminative, and less resource- and time-consuming method for BIC determination. Subsequently, research efforts are needed in this area to find alternative methods for performing this histomorphometric analysis.

Some studies have used CLSM to visualize high-contrast images of bone tissues without the need for sample processing and staining that are required in conventional light microscopy (Grötz et al. 1999; Al-Nawas & Götz 2003a; Orsini et al. 2007). CLSM has also been used to analyze the BIC in several studies (Al-Nawas et al. 2003b, 2008), acquiring the reflected light coming from the implant and from the tissue. In this method, the difference in intensities between both reflecting surfaces was used to distinguish them and later to measure the BIC.

On the other hand, the analysis could be performed in SEM mode with secondary and backscattering electrons. Several studies have been carried out using this technique for surface implant texturization (Marin et al. 2008; Ballo et al. 2009; Kelly et al. 2009; Jeong et al. 2010; Fontana et al. 2011; Johansson et al. 2012; Coelho et al. 2012). Recently, elemental analysis with SEM has been used to evaluate neoformed bone composition with different implant systems (Ballo et al. 2009; Calvo-Guirado et al. 2012). Nevertheless, to our knowledge, the determination of BIC based on SEM methodology has been scarcely reported so far (Chang et al. 2009; Lee et al. 2009; Vidi-gal et al. 2009; Calvo-Guirado et al. 2012).

In the present study, histomorphometric analysis by a new standardized and high discriminative method to quantify BIC based on scanning electron microscopy with backscattered electrons (BS-SEM) imaging is described. The measurements were performed along the total length of the implants, buccal and lingual.

Material and Methods

Animals and surgical procedure
According to the ARRIVE guidelines for reporting the animal experimentation (Kilkenny et al. 2010; Berglundh & Stavropoulos 2012), the animal study was approved by the Animal Experimentation Ethics Committee (AEEC) of the University of Barcelona (UB, Spain). To perform this observational study to describe a new BIC measurement technique, special attention has been paid to both, the reduction in the number of animals and to the reduction in the minimum of their suffering, according to the so-called "3Rs" (Replacement, Refinement, and Reduction of animals in research) as defined by Kilkenny et al. (2010). In this sense, six adult beagle dogs, weighing an average of 11.5 kg, were selected and installed in the animal experimentation service facility of Bellvitge's Health Science Campus of the UB, under veterinary control. All experiments were performed according to the Spanish Government guide (Royal Decree 1201/2005 of October 10th, Spanish Official Gazette 252, October 21st, 2005) and the European guide (European Union Council Directive of November 24th, 1986, 86/609/EEC) for animal use and care. Through the experimental study, all animals were fed with a soft diet, and mechanical cleaning of teeth and implants was performed daily.

All mandibular premolars were extracted bilaterally. After a healing period of 3 months, three implants (9 mm length, Ø 4.0 mm; Biohorizons® Implant Systems INC. Birmingham, AL, USA) with a SBM (sand-blasting with soluble particles) surface were placed in each hemi-mandibular premolar region, according to the protocol suggested by the manufacturer (Biohorizons). The implants were placed at 7 mm distance from each other. A total of 36 implants were placed. All surgical procedures were performed by the same operator (C.M.). The surgical approach occurred under general anesthesia and was supervised by a veterinary surgeon. Once anaesthetized, buccal and lingual full-thickness flap were reflected, and implant placement procedure was carried out according to the manufacturer's instructions. Flaps were sutured using silk 4.0 interrupted sutures and removed after 10 days. After surgery, an intramuscular injection (prophylactically) of Terramycin 100® (25 mg/kg; Pfizer Laboratories, Alcobendas, Spain) was provided. The postoperative analgesia was carried out by the administration of meloxicam (5 mg/ml; 5 mg/ 20 Kg /24 h; Metamecam® injectable solution, Boehringer Ingelhein, Rhein, Germany). Finally, dogs were sacrificed at time points: 0, 1, 2, 4, 6, and 8 weeks after implant installation, by means of an overdose of sodium pentothal. The mandibles were dissected, and each implant site was removed using a diamond saw, so samples could be obtained and prepared for histological analysis.

Specimen preparation and histomorphometric evaluation
The biopsies were processed for ground sectioning (Donath & Breuner 1982; Donath 1985). The implant–bone specimens were fixed in 10% formaldehyde for 1 week and dehydrated in ascending series of alcohol rinses before being embedded without decalcification in light-curing epoxy resin (Technovit®; Exakt-Kultzer, Wahrheim, Germany). Blocks were sectioned buccolingualy with a diamond-edge band saw blade (Exakt micro-parallel-grinding System®; Exakt, Nordenstedt, Germany) and then ground and polished with 1200 and 4000 grain sandpaper to obtain a polished surface. The blocks were coated with evaporated carbon and fixed with colloidal silver; four silver tracks were directed to the region of interest to improve the conductivity of the specimen (Franch et al. 2000).

Image acquisition
Prior to the carbon coating, samples were observed under a Leica MZFLIII stereoscope to ensure the quality of the sectioned blocks. Images were acquired with a Cannon Power-Shot A610 coupled to the stereoscope (Fig. 1a). After the carbon coating, the samples were analyzed using BS-SEM (S-360, Leica, Cambridge, UK), in the Scientific and Technological Centers of the University of Barcelona. All samples were observed in equal conditions (20 mm WD, 50× magnifications, 1 nA and 20 kV), and consecutive pictures (10 to 16 images per sectioned block) with at least 15% of overlap were obtained along the contour of the implant.

Image processing and BIC determination
Image processing and analysis were performed using the Fiji image processing package (http://pacific.mpi-cbg.de/). Images were stitched together with the Fiji stitching plugin (S. Preibisch et al. 2009) to have a composition of the whole section (Fig. 1b). This plugin allowed automatic stitching of all images in a directory, but it also allowed a 2D manual stitching approach when the former did not work properly.

The first step in the image analysis was to segment the implant. To do so, the stitched image was first filtered with a median filter of radius 2 and then thresholded for the maximum gray levels (200–255). This resulted in the binary image of the implant (Fig. 1c). A second step was to force a region of overlap between the implant and the bone. By
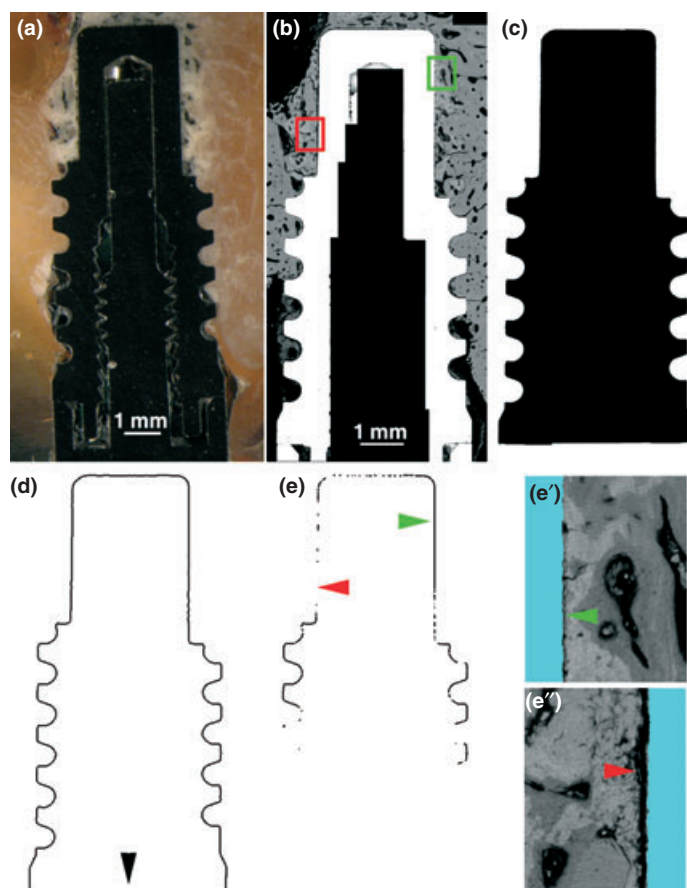
Fig. 1. Bone-to-implant contact (BIC) determination based on backscattered scanning electron microscopy (BS-SEM) images. (a) Stereoscopic image of one sample. (b) Stitched image of 14 BS-SEM images. Observe the difference in intensity between the implant (white) and tissue (gray). (c) Binary image of the segmented implant. (d) Outline of the implant after dilating. The external rim line is removed (black arrowhead). (e) Intersection line between (d) and (b). (e′ and e″) Insets of green (e′) and red (e″) areas in (b). Implant is colored in cyan. Green and red arrowheads in (e–e″) point out a region with and without BIC, respectively. Scale bar: 1 mm.

dilating the binary image six times, six pixels were added to the edges of the implant, enlarging it up to 15 μm on each side. This distance was adjusted to overcome the minimal separation observed between bone and implant (Fig. 1e′), probably due to the strain applied to the polymers embedding the block by the BS-SEM vacuum chamber. Larger distances were considered as absence of BIC (Fig. 1e″). The enlarged implant was finally outlined to generate a one-pixel-wide line (Fig. 1d) around it that was used to intersect the bone in the original image. The overlap between bone and outline was obtained (Fig. 1e) using the Boolean operation Min of the image calculator function of Fiji. This operation gave an image of a one-pixel-wide line where the outline of the implant intersected the bone and where the gray level was the minimum intensity between both. Therefore, the gray levels of the overlapping line were those from the bone, allowing further analysis in case differences in calcium concentration were to be investigated.

Finally, the percentage of BIC (buccolingual) was calculated. The length of the outline of the enlarged implant was considered the maximum possible BIC (100%), and the length of the overlapping line was considered the real BIC. Both measurements were performed after subtraction of the external rim line (Fig. 1d) where BIC is not possible. The percentage of BIC was calculated by dividing the real BIC by the maximum possible BIC and multiplying by 100.

Results and discussion

Backscattered electron (BS-SEM) imaging is a useful technique to assess differences in density for surface areas of calcified tissues, resulting in images with different gray levels (Franch et al. 2000; Roschger et al. 2003). The higher the density for a specific atomic structure of the mineral phase, the more electrons backscattered from the surface region and the brighter the resulting image

(Goldstein et al. 2005). Thus, calcified tissues show a gray level in the images depending on their calcium concentration, whereas the embedding material and the non-calcified tissues appear black (Fig. 1b and Fig. 3). The metallic implant, on the other hand, appears almost saturated at the maximum of the gray scale because of the high density of its titanium alloy.

The main limitation for conventional microscopy is the weaker contrast between the bone and the implant, unless some heavy staining is performed. CLSM, on the other hand, offers the possibility of acquiring images of the surface by detecting its reflection and thus without staining. In this case, a very good contrast between bone and implant is observed due to the high reflection of the implant. Some reflection from the soft tissues and the resin could interfere, however, giving rise to false positives (data not shown).

The method described in this study is based on the high contrast between bone and implant in BS-SEM images. This method offers several important advantages over the classical techniques based on the sawing–grinding processes (Donath & Breuner 1982) and the evaluation of stained thin sections by light microscopy (Abrahamsson et al. 2009; Calvo-Guirado et al. 2011; Santis et al. 2011). First, it avoids the risk of bias as there is no need for staining and the process of image analysis is standardized. Second, BIC measurements are more precise as BS-SEM images have a much higher resolution and a much higher contrast between implant and bone than conventional optical microscopy images. Third, this method allowed the analysis of the whole implant instead of individual areas, thus giving a more complete BIC measurement. However, if the interest is measuring BIC in a specific area, the proposed image analysis method is absolutely adaptable, precise, and robust. Fourth, the BS-SEM microscope can differentiate calcified tissues depending on their calcium concentration. The line where the real BIC was measured could be analyzed differentially based on its intensity levels, depending on the calcium concentration detected in the image. In addition, the morphological characteristics of the calcified tissues, such as the size and shape of the cell's lacunae, and the cementing lines could also be assessed and submitted to quantitative analysis (López-López et al. 2009). Fifth, BS-SEM imaging is non-destructive and therefore allows a posterior histological observation of the samples. Moreover, in comparison with

Table 1. Bone-to-implant contact percentage

Time (weeks)	BS-SEM Median	BS-SEM Mean	SD
0	22.3	24.7	11.64
1	23.4	23.7	4.78
2	25.8	22.9	7.43
4	34.2	36.2	11.54
6	30.0	33.0	16.52
8	44.3	45.5	17.16

SD, standard deviation; BS-SEM, backscattered scanning electron microscopy.

Fig. 2. Mean and median values of BIC% in the eight-week measurement period of the study. Each value corresponds to six implant units. Dashed lines correspond to 95% confidence interval.

the classical methods, the time to process and analyze the samples is reduced. Finally, the method used to measure BIC described in this work could also be applied to images coming from conventional optical microscopy and CLSM.

The results obtained with this methodology of image acquisition, processing, and analysis showed an evolution along time very similar to that obtained by other authors in comparable studies (Klongnoi et al. 2006; Tavares et al. 2007; Abrahamsson et al. 2009; Ballo et al. 2009; Calvo-Guirado et al. 2011; Santis et al. 2011). The mean of the percentages of BIC measurements for each time point are depicted in Table 1 and Fig. 2. In the first periods, from time 0 to week 2, the percentage of BIC was <30%. Images corresponding to those values and timing showed that the calcified tissues around the implant were immature and surrounded by vascular spaces (Fig. 3a–c). From the 4th week, the percentage of BIC clearly increased up to the last time point of the experiment (8 weeks). Images at the 4th week showed a higher level of contact between the implant and a denser osseous structure with fewer and smaller vascular spaces and more mature bone tissue (Fig. 3d). At weeks 6 and 8, the increase in the percentage of BIC was in parallel with the increase in maturity of the osseous tissue that gradually surrounded the implant surface (Fig. 3e,f).
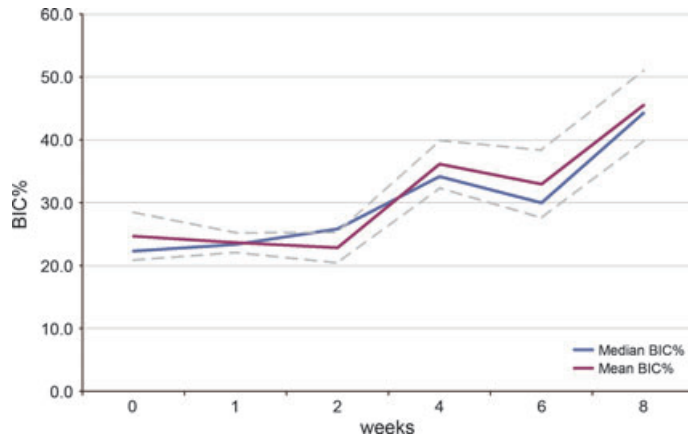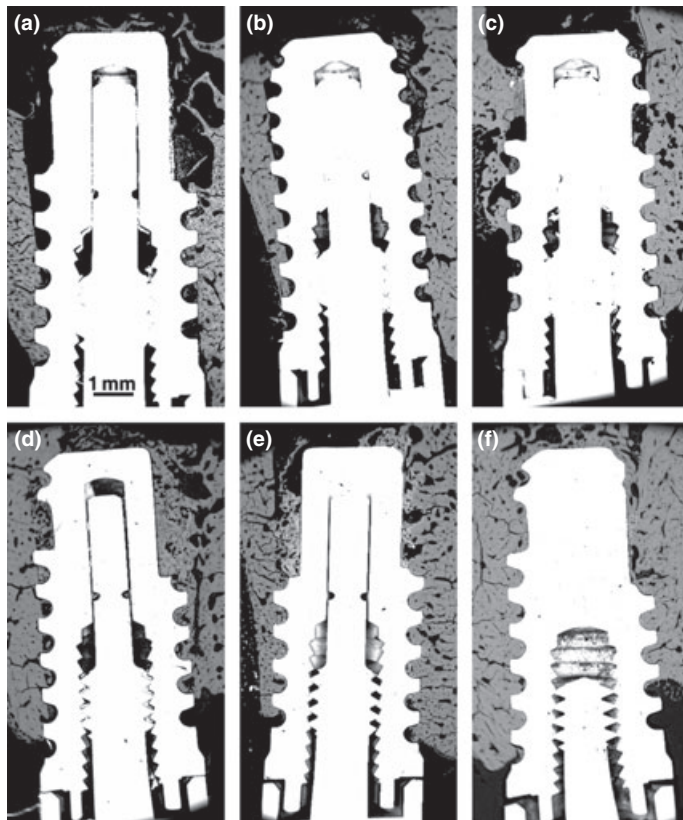
Conclusions

A novel method for measuring BIC based on BS-SEM images is described. The obtained images offer an excellent contrast between bone and implant, which allows the images to be processed for measuring the BIC in an objective, systematic, and high discriminative way. Another advantage is that the time to process the samples is reduced with regard to the classical method of measuring BIC. As the proposed method is a non-destructive one, it allows a posterior histological observation of the samples. The percentage of BIC achieved with the novel method was similar to the values documented in the literature for implants of similar roughness in animal models.

References

Abrahamsson, I., Linder, E. & Lang, N.P. (2009) Implant stability in relation to osseointegration: an experimental study in the Labrador dog. *Clinical Oral Implants Research* **20**: 313–318.

Al-Nawas, B. & Götz, H. (2003a) Three-dimensional topographic and metrologic evaluation of dental implants by confocal laser scanning microscopy. *Clinical Implant Dentistry and Related Research* **5**: 176–183.

Al-Nawas, B., Götz, H., Grötz, K.A. & Duschner, H. (2003b) Standardized characterization of

Fig. 3. Progression of bone-to-implant contact (BIC). (a–f) Backscattered scanning electron microscopy images of different implants at 0, 1, 2, 3, 4, 6, and 8 weeks, respectively. Observe the increase in the BIC along time. All images at the same scale.

peri-implant bone structure using confocal laser scanning microscopy (CLSM). *European Cells and Materials IV* **5**: 53.

Al-Nawas, B., Groetz, K.A., Goetz, H., Duschner, H. & Wagner, W. (2008) Comparative histomorphometry and resonance frequency analysis of implants with moderately rough surfaces in a loaded animal model. *Clinical Oral Implants Research* **19**: 1–8.

Ballo, A.M., Akca, E.A., Ozen, T., Lassila, L., Vallittu, P.K. & Närhi, T.O. (2009) Bone tissue responses to glass fiber-reinforced composite implants - A histomorphometric study. *Clinical Oral Implants Research* **20**: 608–615.

Berglundh, T. & Stavropoulos, A. (2012) Preclinical in vivo research in implant dentistry. Consensus of the eighth european workshop on periodontology. *Journal of Clinical Periodontology* **39**: 1–5.

Calvo-Guirado, J.L., Aguilar-Salvatierra, A., Guardia, J., Delgado-Ruiz, R., Ramírez-Fernández, M.P., Pérez Sánchez, C. & Gómez-Moreno, G. (2012) Evaluation of periimplant bone neoformation using different scanning electron microscope methods for measuring BIC. A dog study. *Journal of Clinical and Experimental Dentistry* **4**: e8–e13.

Calvo-Guirado, J.L., Mate-Sanchez, J., Delgado-Ruiz, R., Ramirez-Fernández, M.P., Cutando-Soriano, A. & Peña, M. (2011) Effects of growth hormone on initial bone formation around dental implants: a dog study. *Clinical Oral Implants Research* **22**: 587–593.

Chang, C.-S., Lee, T.-M., Chang, C.-H. & Liu, J.-K. (2009) The effect of microrough surface treatment on miniscrews used as orthodontic anchors. *Clinical Oral Implants Research* **20**: 1178–1184.

Coelho, P.G., Marin, C., Granato, R., Giro, G., Suzuki, M. & Bonfante, E.A. (2012) Biomechanical and histologic evaluation of non-washed resorbable blasting media and alumina-blasted/acid-etched surfaces. *Clinical Oral Implants Research* **23**: 132–135.

Donath, K. (1985) The diagnostic value of the new method for the study of undecalcified bones and teeth with attached soft tissue (sage-schliff (sawing and grinding) technique). *Pathology Research and Practice* **179**: 631–633.

Donath, K. & Breuner, G. (1982) A method for the study of undecalcified bones and teeth with attached soft tissues. the sage-schliff (sawing and grinding) technique. *Journal of Oral Pathology* **11**: 318–326.

Fontana, F., Rocchietta, I., Addis, A., Schupbach, P., Zanotti, G. & Simion, M. (2011) Effects of a calcium phosphate coating on the osseointegration of endosseous implants in a rabbit model. *Clinical Oral Implants Research* **22**: 760–766.

Franch, J., Pastor, J., Franch, B., Durall, I., Manzanares, M.C. & Feline, J. (2000) Back-scattered electron imaging of a non-vertebral case of hypervitaminosis A in a cat. *Journal of Feline Medicine and Surgery* **2**: 49–56.

Goldstein, J., Newbury, D.E., Joy, D.C., Echlin, P., Roming, A.D., Lyman, C.E., Fiori, C. & Lifshin, E. (2005) Scanning Electron Microscopy and X-Ray Microanalysis. New York, NY: Kluwer Academic/Penum Publishers.

Grötz, K.A., Piepkorn, B., Al-Nawas, B., Duschner, H., Bittinger, F., Kann, P., Beyer, J. & Wagner, W. (1999) Confocal laser scanning microscopy: a non-destructive subsurface histotomography of healthy human bone. *Calcified Tissue International* **65**: 8–10.

Jeong, R., Marin, C., Granato, R., Suzuki, M., Gil, J.N., Granjeiro, J.M. & Coelho, P.G. (2010) Early bone healing around implant surfaces treated with variations in the resorbable blasting media method. A study in rabbits. *Medicina Oral Patologia Oral y Cirugia Bucal* **15**: e119–e125.

Johansson, C.B., Gretzer, C., Jimbo, R., Mattisson, I. & Ahlberg, E. (2012) Enhanced implant integration with hierarchically structured implants: a pilot study in rabbits. *Clinical Oral Implants Research* **23**: 943–953.

Kelly, J., Lin, A., Wang, C.J., Park, S. & Nishimura, I. (2009) Vitamin D and bone physiology: demonstration of vitamin D deficiency in an implant osseointegration rat model. *Journal of Prosthodontics* **18**: 473–478.

Kilkenny, C., Browne, W.J., Cuthill, I.C., Emerson, M. & Altman, D.G. (2010) Improving bioscience research reporting: the ARRIVE guidelines for reporting animal research. *Journal of Pharmacology and Pharmacotherapeutics* **1**: 94–99.

Klongnoi, B., Rupprecht, S., Kessler, P., Thorwarth, M., Wiltfang, J. & Schlegel, K.A. (2006) Influence of platelet-rich plasma on a bioglass and autogenous bone in sinus augmentation: an explorative study. *Clinical Oral Implants Research* **17**: 312–320.

Lee, J., Sieweke, J.H., Rodriguez, N.A., Schupbach, P., Lindstrom, H., Susin, C. & Wikesjö, U.M. (2009) Evaluation of nano-technology-modified zirconia oral implants: a study in rabbits. *Journal of Clinical Periodontology* **36**: 610–617.

López-López, J., Chimenos-Küstner, E., Manzanares-Cespedes, C., Muñoz-Sánchez, J., Castañeda-Vega, P., Jané-Salas, E., Alvarez-López, J.M. & Gimeno-Sanding, A. (2009) Histomorphological study of the bone regeneration capacity of platelet-rich plasma, bone marrow and tricalcium phosphate: experimental study on pigs. *Medicina Oral Patología Oral y Cirugía Bucal* **14**: e620–e627.

Marin, C., Granato, R., Suzuki, M., Gil, J.N., Piattelli, A. & Coelho, P.G. (2008) Removal torque and histomorphometric evaluation of bioceramic grit-blasted/acid-etched and dual acid-etched implant surfaces: an experimental study in dogs. *Journal of Periodontology* **79**: 1942–1949.

Orsini, G., Piattelli, M., Scarano, A., Petrone, G., Kenealy, J., Piattelli, A. & Caputi, S. (2007) Randomized, controlled histologic and histomorphometric evaluation of implants with nanometer-scale calcium phosphate added to the dual acid-etched surface in the human posterior maxilla. *Journal of Periodontology* **78**: 209–218.

Preibisch, S., Saalfeld, S. & Tomancak, P. (2009) Globally optimal stitching of tiled 3D microscopic image acquisitions. *Bioinformatics* **25**: 1463–1465.

Roschger, P., Gupta, H.S., Berzlanovich, A., Ittner, G., Dempster, D.W., Fratzl, P., Cosman, F., Parisien, M., Lindsay, R., Nieves, J.W. & Klaushofer, K. (2003) Constant mineralization density distribution in cancellous human bone. *Bone* **32**: 316–323.

Santis, E.D., Botticelli, D., Pantani, F., Pereira, F.P., Beolchini, M. & Lang, N.P. (2011) Bone regeneration at implants placed into extraction sockets of maxillary incisors in dogs. *Clinical Oral Implants Research* **22**: 430–437.

Tavares, M.G., Tambasco De Oliveira, P., Nanci, A., Hawthorne, A.C., Rosa, A.L. & Xavier, S.P. (2007) Treatment of a commercial, machined surface titanium implant with H2SO4/H2O2 enhances contact osteogenesis. *Clinical Oral Implants Research* **18**: 452–458.

Vidigal, G.M., Groisman, M., Gregório, L.H. & Soares, G.D.A. (2009) Osseointegration of titanium alloy and HA-coated implants in healthy and ovariectomized animals: a histomorphometric study. *Clinical Oral Implants Research* **20**: 1272–1277.